



**HAL**  
open science

## Retinal Optical Coherence Tomography: Past, Present and Future Perspectives

Wolfgang Geitzenauer, Cristoph K Hitzenberger, Ursula M Schmidt-Erfurth

► **To cite this version:**

Wolfgang Geitzenauer, Cristoph K Hitzenberger, Ursula M Schmidt-Erfurth. Retinal Optical Coherence Tomography: Past, Present and Future Perspectives. *British Journal of Ophthalmology*, 2010, 95 (2), pp.171. 10.1136/bjo.2010.182170 . hal-00560855

**HAL Id: hal-00560855**

**<https://hal.science/hal-00560855>**

Submitted on 31 Jan 2011

**HAL** is a multi-disciplinary open access archive for the deposit and dissemination of scientific research documents, whether they are published or not. The documents may come from teaching and research institutions in France or abroad, or from public or private research centers.

L'archive ouverte pluridisciplinaire **HAL**, est destinée au dépôt et à la diffusion de documents scientifiques de niveau recherche, publiés ou non, émanant des établissements d'enseignement et de recherche français ou étrangers, des laboratoires publics ou privés.

## TITLE PAGE

**TITLE:**

Retinal Optical Coherence Tomography: Past, Present and Future Perspectives

**CORRESPONDING AUTHOR:**

Prof. Ursula M Schmidt-Erfurth, MD

Dept. of Ophthalmology

Medical University of Vienna

Waehringer Guertel 18-20

1090 Vienna

Austria

E-Mail: [ursula.schmidt-erfurth@meduniwien.ac.at](mailto:ursula.schmidt-erfurth@meduniwien.ac.at)

Tel: +43-1-40400-7931

Fax: +43-1-40400-7932

**CO-AUTHORS:**

Wolfgang Geitzenauer, MD

Dept. of Ophthalmology

Medical University of Vienna

Vienna, Austria

Prof. Christoph Hitzenberger, PhD

Center for Medical Physics and Biomedical Engineering

Medical University of Vienna

Vienna, Austria

**KEYWORDS:**

Optical Coherence Tomography

Imaging

Time Domain

Spectral Domain

**WORD COUNT:**

3.574 words

2 **Abstract**

3

4 Optical coherence tomography (OCT) has undergone substantial changes since its  
5 first use in the 1990s. Although the first generation of OCT systems heralded a new  
6 era in the non-invasive diagnostic options in ophthalmology, they did not reveal much  
7 detail. Later devices offered more information and helped further in the diagnosis and  
8 treatment of a variety of pathologic conditions primarily of the retina. With today's  
9 spectral-domain type models ophthalmologists are offered a comprehensive tool with  
10 the opportunity for early diagnosis and precise monitoring of patients with retinal and  
11 glaucomatous pathologies. However, as experience with these new devices grows and  
12 demands by clinicians and researchers raise, further improvements need to be  
13 addressed. Future developments in the improvement of the transverse resolution and  
14 extension of the penetration depth are to be expected. New modalities such as  
15 polarization sensitive OCT (PS OCT) or Doppler OCT have been used already in the  
16 recent past and promise additional insights in the properties of physiologic and  
17 pathologic tissue. While PS OCT reveals further detail in alterations of the retinal  
18 pigment epithelium, Doppler OCT gives additional information about blood flow  
19 measurements. With these and further new developments OCT will continue to be an  
20 invaluable instrument in the armamentarium of modern ophthalmology.

21

22 **Licence statement:**

23 The Corresponding Author has the right to grant on behalf of all authors and does  
24 grant on behalf of all authors, an exclusive licence (or non-exclusive for government  
25 employees) on a worldwide basis to the BMJ Publishing Group Ltd and its Licensees  
26 to permit this article (if accepted) to be published in British Journal of Ophthalmology  
27 and any other BMJ PGL products to exploit all subsidiary rights, as set out in our  
28 licence.

29

30 **Competing interest:**

31 The authors' employer, the Medical University of Vienna, received funding from Carl  
32 Zeiss Meditec and Heidelberg Engineering for sponsored projects by the Department  
33 of Ophthalmology.

34 Wolfgang Geitznauer: received reimbursements for honoraria for presentations at  
35 meetings from Carl Zeiss Meditec and Heidelberg Engineering.

36 Ursula Schmidt-Erfurth: none to declare.

37 Christoph Hitzenberger: none to declare.

38

39 **Retinal Optical Coherence Tomography: Past, Present and Future Perspectives**

40

41 **Introduction**

42

43 Optical coherence tomography (OCT), a widely used technology in clinical routine  
44 and ophthalmic research, has been used since the 1990s. The basis for future  
45 developments of OCT in ophthalmology were measurements of the eye length by  
46 laser interferometry.[1-2] The first ophthalmic imaging by OCT was reported by

47 Huang and co-workers in 1991.[3] At this time, the application of OCT was  
48 demonstrated in retinal and vascular tissue. Two years later the first in vivo images of  
49 the retina were published.[4-5] Within a few years only substantial progress has been  
50 made with regard to both axial and transverse resolution as well as in the everyday  
51 practical usability. Today, OCT is a well established tool in the diagnosis of retinal  
52 diseases, glaucoma and in the evaluation of anterior-segment conditions. The recent  
53 success of new drugs for the management of retinal diseases such as age-related  
54 macular degeneration (AMD) and diabetic macular oedema (DME) has been boosted  
55 by improvements in OCT technology.

56

### 57 **Optical Coherence Tomography: Past**

58

59 The step forward from ultrasonography to a non-invasive, in vivo examination of  
60 cross-sectional images of retinal tissue based on the reflectivity of backscattered light  
61 was greatly welcomed by the ophthalmic community. Low-coherence interferometry  
62 as the general principle of OCT has been described elsewhere in detail.[1-2] The use  
63 of super luminescent diodes (SLD) as affordable and compact light sources facilitated  
64 greatly the dissemination of commercial systems. The coherence of the reflected or  
65 backscattered light is used for measuring the position of backscattering sites. The first  
66 commercially available systems were based on time-domain technology (TD-OCT),  
67 produced by Humphrey Instruments, Inc. and released in 1995 (OCT 1). The latest  
68 instrument based on this type of technology was the Stratus OCT (Carl Zeiss Meditec,  
69 Inc.).

70 From today's perspective images from both OCT 1 and OCT 2 systems did not reveal  
71 much detail. However, until the introduction of the Stratus OCT system the

72 information given was unprecedented and allowed objective documentation that had  
73 previously not been possible. False-colour coded reflectivities made the internal  
74 limiting membrane (ILM) and retinal pigment epithelium (RPE) recognisable but did  
75 not show much detail. OCT 2 offered some minor hardware and ergonomic  
76 improvements at its release in 2001. Both instruments were able to capture 100 axial  
77 measurements in one second and had an axial resolution of ~ 15 micrometers.  
78 Although pupil dilation was a critical necessity, fundamental new insights in the  
79 disease pathogenesis and specifications, particularly in patients with macular  
80 edema[6-7], macular holes[8-12], and vitreomacular traction syndrome[10, 13] were  
81 gained with these early OCT models. Application in glaucoma has been reported from  
82 the beginning of OCT in ophthalmology[14] but was limited until the widespread use  
83 of the Stratus OCT.

84 The underlying principle used was the time-domain technique, referring to the  
85 sequential capture of information along the axis of the light beam. By using this  
86 technology, the Stratus OCT with its image acquisition speed of 400 axial scans per  
87 second was able to acquire up to 768 adjacent A-scans with an axial resolution of up  
88 to 10 micrometers. The information was then presented as one virtual cross-sectional  
89 B-scan with false-colour coding according to the relative signal strength of the  
90 backscattered light. Six radial line scans were then interpolated to calculate the retinal  
91 thickness of the scanned area. Similarly, single-line circular optic nerve head scans  
92 could be produced.[14] Due to the relatively low acquisition speed of the TD-OCT  
93 motion and blinking artefacts were often inevitable.

94 The transition to Fourier-domain (or spectral-domain) technology together with newly  
95 available light sources led to enhancements in acquisition speed, sensitivity and  
96 resolution. [15-19]

97

98 **Optical Coherence Tomography: Present**

99

100 One characteristic of the latest generation OCT technology (i.e. SD-OCT or FD-OCT)  
101 is its higher acquisition speed with up to 40,000 axial scans per second in commercial  
102 systems. Additional optional features such as averaging of multiple scans to reduce  
103 speckle noise[20-21] and real-time tracking to account for eye-movements[22-23]  
104 have further enhanced image quality. These features are already available in a  
105 commercial system (Heidelberg Spectralis) and can be used to average several images  
106 recorded at exactly the same location, or to record exactly the same location on  
107 successive visits, thus improving the reliability of quantitative imaging in follow-up  
108 studies. Although improvements in image resolution had been achieved already with  
109 time-domain systems in experimental settings[24], it was spectral-domain technology  
110 that made such improvements available in commercial instruments. Current  
111 limitations are 2 to 3 micrometers in experimental systems[25-26] and around 5  
112 micrometers in commercial systems. Interpolation between single scans was  
113 dramatically reduced and therefore an important source of bias in the volumetric  
114 measurements eliminated.

115

116 With volumetric datasets available, visualisation and processing of three-dimensional  
117 renderings have been investigated extensively (Figure 1).[27-30] In addition to  
118 standard B-scan imaging, C-scans (en-face images) and arbitrary oriented sectional  
119 images can be derived from the 3D data sets. Segmentation, i.e. identification and  
120 delineation of selected layers such as the ILM, nerve fibre layer (NFL), inner/outer  
121 photoreceptor segment junction and the RPE is another important feature of SD-OCT

122 technology.[31-33] Crucial to the development and the precision of automatic  
123 detection of retinal layers by software algorithms is high image quality, i.e. a low  
124 level of noise and a reduction of motion-induced image distortions. Algorithm  
125 failures, a phenomenon well-known in older generation OCT systems[34-35], are  
126 strongly related to poor image quality.

127

128 Retinal changes associated with age-related macular degeneration (AMD) have been  
129 examined extensively with OCT earlier, but with the introduction of pharmacological  
130 therapy and the antipermeability effect of antiangiogenic substances, OCT became the  
131 most important tool in therapeutic follow-up.[36-37] It became possible to monitor  
132 central retinal thickening and to detect intra- and subretinal changes that were not  
133 recognised ophthalmoscopically or by angiography.[38-39] One small study[36]  
134 followed by large multi-centre drug trials (SUSTAIN trial[40], SAILOR trial[41])  
135 have established the use of OCT for the indication of retreatment with recently  
136 available anti-VEGF drugs, a development that supports the role of OCT for disease  
137 monitoring and indication of treatment in AMD. The appearance of macular cysts or  
138 subretinal fluid in the macula after anti-VEGF therapy was assumed to represent an  
139 early sign of CNV recurrence. For future studies Fung and co-workers suggested an  
140 approach oriented on those qualitative changes on the OCT images as an indicator for  
141 retreatment. The EXCITE trial[42] followed this approach and compared the efficacy  
142 and safety of two different dosing regimens of ranibizumab to evaluate the role of  
143 OCT as a retreatment indicator in neovascular AMD. Positive correlation between  
144 OCT findings and disease activity demonstrated by fluorescein angiography has been  
145 shown in patients with AMD during retreatments of photodynamic therapy.[43-44]

146

147 However, the role of OCT at the initial diagnostic stage is currently still  
148 complementary to angiography. Although extensive knowledge about the  
149 microstructural retinal changes in certain diseases has been gained it is important to  
150 emphasise that differential diagnostic considerations at the initial stage of diagnosis  
151 cannot be made solely based on OCT.

152 Retinal thickness was initially introduced as a marker for disease severity. However,  
153 differentiation between intraretinal and subretinal fluid accumulation can reveal more  
154 disease-specific insights in natural course and treatment effects of retinal  
155 subcompartments.[45] Ahlers and co-workers showed different time-courses of  
156 treatment effects after intravitreal ranibizumab according to its anatomical location,  
157 with sub-retinal fluid and pigment-epithelium detachment reduction occurring early  
158 during follow-up, whereas the total retinal volume (ILM to RPE) decrease was noted  
159 over the full observation period of three months.

160  
161 Central 1 mm retinal thickness has been regarded as the ideal morphologic correlate to  
162 visual function in the majority of previous studies. Only recently it was shown that  
163 there is not necessarily a strong correlation between both parameters.[46-47] Similar  
164 findings were reported in functional aspects of macular holes, where the condition of  
165 the external limiting membrane as seen on SD-OCT cross-sectional images and three-  
166 dimensional renderings was found to be a predictor of the integrity of the junction  
167 zone of the inner and outer segments of the photoreceptors.[48] These findings  
168 certainly have an influence on future characterisation and information about the  
169 postoperative functional gain that can be achieved.

170

171 The introduction of SD-OCT into clinical ophthalmology represents a major  
172 methodological enhancement that has been welcomed by both researchers and  
173 clinicians. Although first results have just been published in the last two years and  
174 experience is limited, there is certainly a potential for further improvement, e.g. noise  
175 reduction and algorithm performance. Mapping of the ganglion cell complex as  
176 demonstrated by Tan et al. has significantly contributed to glaucoma diagnosis and  
177 monitoring.[49] Though originally developed with older generation OCT systems this  
178 functionality is commercially available with SD-OCT.

179 Additional layers beyond the currently available segmentations of the ILM and RPE  
180 are already implemented in research software applications and can therefore be  
181 expected to be available soon to the clinician.

182

### 183 **Future perspectives**

184

185 A large variety of novel and advanced OCT technologies are presently under  
186 development. We provide a short overview of the most promising of these techniques.

187

#### 188 *Improved transverse resolution*

189 Contrary to other optical imaging techniques, axial and transverse resolution are  
190 decoupled in OCT. Axial resolution is determined by the source bandwidth, lateral  
191 resolution by the numerical aperture of the system. Initially, development was focused  
192 on axial resolution, providing ~ 5  $\mu\text{m}$  for commercial SD-OCT systems and 2-3 for  
193 special research instruments [50]. Transverse resolution, however, is still limited to ~  
194 15 – 20  $\mu\text{m}$  in commercial systems.

195 Transverse resolution is determined by the beam spot size on the retina which depends  
196 on the numerical aperture and on aberrations of the ocular refractive media. For  
197 retinal OCT, the numerical aperture is limited by the maximum iris diameter of ~ 7  
198 mm. However, beam sizes of this diameter can normally not be used because of  
199 wavefront aberrations caused by the eye. Commercial retinal OCT instruments  
200 typically use beam diameters of the order of ~ 1 mm, limiting the transverse  
201 resolution to ~ 20  $\mu\text{m}$ .

202 This limitation can be overcome in two steps. For eyes with low aberrations, the beam  
203 diameter can be expanded to ~ 3-4 mm, yielding a transverse resolution of ~ 5 – 7  $\mu\text{m}$ ,  
204 sufficient to image cone photoreceptors at an eccentricity of  $\sim 4^\circ$  or larger[51].

205 A further increase of the beam diameter degrades transverse resolution because  
206 excessive wavefront aberrations increase the spot size on the retina. This can be  
207 overcome by adaptive optics (AO), which measures wave front distortions by a wave  
208 front sensor and corrects for the distortions by a deformable mirror. First applications  
209 of AO to OCT were reported just a few years ago[52-53], the first successful images  
210 of human cone photoreceptors were demonstrated in 2005[54]. AO-OCT is rapidly  
211 developing and different variants were reported[55-63], finally achieving a nearly  
212 isotropic resolution of 2-3  $\mu\text{m}$  in axial and lateral directions [64-65], allowing to  
213 resolve cone photoreceptors in the human retina as close as  $\sim 1^\circ$  to the fovea. An  
214 overview of AO-OCT can be found in a recent review[66].

215

#### 216 *Extended penetration depth*

217 Commercial retinal OCT scanners presently operate at wavelengths of ~ 800 nm, for  
218 which a good selection of useful light sources is available. While OCT at 800 nm  
219 provides high-quality images of retinal layers down to the RPE, the penetration into

220 deeper structures is usually poor because of the strong absorption and scattering by  
221 melanin in the RPE. Two approaches towards imaging of deeper layers like choroid  
222 and inner parts of the sclera have been reported. The first approach is based on  
223 commercially available SD-OCT in the 800 nm regime.[67] By positioning the SD-  
224 OCT device close enough to the eye to obtain an inverted representation of the  
225 fundus, the maximum sensitivity of SD-OCT near the zero delay line can be placed  
226 into the deeper layers, providing increased sensitivity for these weak-signal regions.  
227 Furthermore, by exploiting the eye-tracking feature of the Heidelberg Spectralis  
228 system, 100 B-scans are averaged, providing greatly improved signal-to-noise ratio.  
229 The combination of these two measures enabled measurement of choroidal thickness  
230 in healthy and diseased eyes.[68-69]

231 The second approach exploits the fact that the light attenuation by the RPE is  
232 wavelength dependent, longer wavelengths at ~ 1050 nm that are less absorbed and  
233 scattered are presently explored. A first TD-OCT setup demonstrated increased  
234 penetration into the choroid for 1050 nm, as compared to 800 nm OCT[70]. Faster  
235 and more sensitive SD-OCT instruments were subsequently developed, employing  
236 either a spectrometer based approach[71] or the related swept source (SS) OCT  
237 technology[72-73]. With the latter technique, record imaging speeds of up to 249 kA-  
238 scans/s were reported [74]. While increased penetration depth and, with SS-OCT, less  
239 sensitivity decay with depth are the advantages of 1050 nm OCT, the drawback is the  
240 reduced resolution because of the longer center wavelength and smaller usable  
241 bandwidth (because of increased water absorption at 1000 nm and above 1100 nm, a  
242 maximum bandwidth of ~ 60 – 80 nm is usable at the retina, yielding an optimum  
243 axial resolution of ~ 5  $\mu\text{m}$  in retinal tissue).

244

245 *Polarization sensitive OCT*

246 Presently available commercial OCT measures backscattered intensity. While  
247 intensity based OCT can resolve retinal layers very well, it cannot directly  
248 differentiate tissues. However, the light's polarization state can be changed by various  
249 light-tissue interactions and thus be used to generate tissue specific contrast. These  
250 effects are used by polarization sensitive (PS) OCT [75-76]. With PS-OCT, the  
251 sample is typically illuminated either with circularly polarized light or with different  
252 polarization states successively, and the backscattered light is detected in two  
253 orthogonal polarization channels. Initially implemented as TD-OCT [75-77], PS-OCT  
254 techniques were later adapted to SD-OCT [78-80], finally providing ocular imaging  
255 with similar speeds as intensity based SD-OCT [79-81]. Two polarization changing  
256 light-tissue interaction mechanisms are of special interest: birefringence and  
257 depolarization. Birefringence is found in fibrous tissues (from birefringence);  
258 depolarization can be caused by multiple light scattering at large particles or  
259 scattering at non-spherical particles [82].

260 Ophthalmic applications of PS-OCT were demonstrated in the anterior segment and in  
261 the retina. Because of spatial restrictions, we restrict this report to retinal applications,  
262 the majority of reported work. Using PS-OCT, the structures of the ocular fundus  
263 could be classified into polarization preserving (e.g. photoreceptor layer), birefringent  
264 (e.g. retinal nerve fiber layer (RNFL), Henle's fiber layer, sclera, scar tissue) [79, 83-  
265 87], and polarization scrambling or depolarizing (e.g. retinal pigment epithelium  
266 (RPE), choroidal nevus) [79, 85-88]. The results of these studies indicate two possible  
267 future applications of PS-OCT for diagnostics of ocular diseases: A recent animal  
268 study has shown that a damage of the optic nerve leads to a reduced RNFL  
269 birefringence before RNFL thickness changes are detectable by intensity based OCT

270 [89]. Since depth resolved retardation measurements by PS-OCT directly provide  
271 quantitative information on RNFL birefringence [81, 84, 90-91], glaucoma induced  
272 RNFL damage might be detected at an early stage, possibly improving glaucoma  
273 diagnostics. The depolarization caused by the RPE can directly be used to identify and  
274 visualize [86-87, 92], and segment [31] this layer whose integrity is decisive for  
275 photoreceptor metabolism and therefore for visual function. Therefore, PS-OCT is an  
276 interesting tool for diagnosis and follow-up studies of diseases associated with RPE  
277 alterations like AMD.

278 Figure 2 shows an example of B-scans obtained by a PS-OCT instrument in a healthy  
279 human fovea. Fig. 2A shows the conventional intensity image where the three  
280 strongly reflecting boundaries of the posterior retina are marked (IS/OS, boundary  
281 between inner and outer photoreceptor segments; ETPR, end tips of photoreceptors;  
282 RPE, retinal pigment epithelium). The retardation image (Fig. 2B) shows the different  
283 polarizing properties of retinal tissue in this region: most tissues preserve the  
284 polarization state, i.e. do not introduce or change retardation (blue colors), only the  
285 RPE scrambles the polarization state, generating random retardation values (the mix  
286 of all color values appears green in this presentation). Fig. 2C shows the degree of  
287 polarization uniformity (DOPU), which is high (orange to red colors) in all layers  
288 except the RPE. This information was used to segment the RPE and to generate an  
289 overlay image showing intensity (gray scale) and the segmented RPE in red (Fig. 2D).

290 Figure 3 shows an example of a PS-OCT B-scan obtained in the retina of a patient  
291 with AMD. A large atrophy is visible on the left hand side of the image, discernible  
292 by the increased light penetration into deeper layers in the intensity image (Fig. 3A).  
293 Figs. 3B and 3C show the DOPU and the overlay image (segmented RPE in red),  
294 clearly showing the atrophy.

295

296 *Doppler OCT and related methods*

297 Similar to other medical imaging techniques like ultrasound imaging, OCT can also  
298 provide velocity information by exploiting the Doppler effect and related  
299 mechanisms. This technique, called Doppler OCT (DOCT) or optical Doppler  
300 tomography (ODT), was first reported in 1995[93]. Its main application is blood flow  
301 measurement and imaging, and a great variety of different implementations, both in  
302 time[94-95] and spectral domain[96-97], have been reported, providing sensitivities  
303 down to the order of 10  $\mu\text{m/s}$ . A comprehensive overview of all these techniques is  
304 beyond the scope of this review.

305 DOCT is presently a very active research area, and we would like to highlight some of  
306 the most relevant developments for retinal imaging. An important application of  
307 DOCT could be to use blood velocity as a contrast agent for visualization of the  
308 vasculature in the ocular fundus. In this application, the phase changes caused by  
309 moving blood cells are used to differentiate them from the surrounding stationary  
310 tissue and thereby segment the vessels. This technique was called optical coherence  
311 angiography[98-99] and can be used for 3D display of the vessel structure and, e.g.,  
312 used to differentiate retinal from choroidal vessels. Compared to fluorescein  
313 angiography, DOCT has the advantage of not requiring the injection of a contrast  
314 agent, however, has the drawback of being sensitive only to moving blood; vascular  
315 leakage cannot be imaged by this method.

316 Quantitative measurement of the absolute velocity of the moving blood cells, and  
317 perfusion measurements providing blood volume flow are still challenging. To obtain  
318 absolute velocities, details of the vessel geometry have to be known because DOCT  
319 measures only the velocity component parallel to the probing light beam. Recent

320 improvements of retinal DOCT extracted this geometric information from OCT  
321 intensity data[100-101] or developed new probing schemes eliminating orientation  
322 sensitivity by employing two differently oriented beams simultaneously[102]. A first  
323 repeatability study of total retinal blood flow using the former method in 8 healthy  
324 eyes demonstrated a mean coefficient of variation of 10.5 %.[103]

325 Finally, new advanced interferometric schemes should be mentioned that, by  
326 hardware manipulation of the reference or sample beam phase during measurement,  
327 provide superior separation of intensity and flow data and/or access flow speeds that  
328 are beyond the range of conventional DOCT[104-106].

329

330 In ophthalmology, OCT technology has clearly introduced a diagnostic revolution.  
331 The unique feature of a non-invasive modality able to image in an in-vivo approach  
332 retinal structures in detail presents OCT as the ideal modality for detection of early  
333 disease in screening and prevention, for differential diagnosis of various macular  
334 diseases of vascular, degenerative, or inflammatory nature and most importantly to  
335 quantify therapeutic effects and identify recurrence during follow-up. Improved  
336 imaging features such as higher resolution, reliable algorithm for automated  
337 segmentation and selective imaging of relevant layers such as NFL and RPE will  
338 enhance the spectrum of indications and clinical value. The practicality of OCT in  
339 respect to data acquisition e.g. by eye tracking systems and particularly in terms of  
340 archiving of large data volumes and presentation in a user friendly way requires  
341 further improvement to facilitate the establishment in clinical practice. With high-  
342 resolution, three-dimensional OCT ophthalmologists have been offered a technology  
343 which allows an unprecedented insight into the pathophysiology of retinal disease.  
344 For the optimal benefit in favour of our patients it is now necessary to identify the

345 parameters which are clinically relevant i.e. are associated with visual function to  
346 correlate morphology and function and to share the knowledge with the large  
347 ophthalmological community so that the advantages in diagnosis and treatment  
348 become available to universities and community hospitals as well as practices around  
349 the world.

350

351

352 References  
353

- 354 1. Fercher, A.F., K. Mengedoht, and W. Werner, *Eye-Length Measurement by*  
355 *Interferometry with Partially Coherent-Light*. Optics Letters, 1988. **13**(3): p.  
356 186-188.
- 357 2. Hitzenberger, C.K., *Optical measurement of the axial eye length by laser*  
358 *Doppler interferometry*. Invest Ophthalmol Vis Sci, 1991. **32**(3): p. 616-24.
- 359 3. Huang, D., et al., *Optical coherence tomography*. Science, 1991. **254**(5035): p.  
360 1178-81.
- 361 4. Fercher, A.F., et al., *In vivo optical coherence tomography*. Am J Ophthalmol,  
362 1993. **116**(1): p. 113-4.
- 363 5. Swanson, E.A., et al., *In-Vivo Retinal Imaging by Optical Coherence*  
364 *Tomography*. Optics Letters, 1993. **18**(21): p. 1864-1866.
- 365 6. Hee, M.R., et al., *Quantitative assessment of macular edema with optical*  
366 *coherence tomography*. Arch Ophthalmol, 1995. **113**(8): p. 1019-29.
- 367 7. Puliafito, C.A., et al., *Imaging of macular diseases with optical coherence*  
368 *tomography*. Ophthalmology, 1995. **102**(2): p. 217-29.
- 369 8. Hee, M.R., et al., *Optical coherence tomography of macular holes*.  
370 Ophthalmology, 1995. **102**(5): p. 748-56.
- 371 9. Gaudric, A., et al., *Macular hole formation: new data provided by optical*  
372 *coherence tomography*. Arch Ophthalmol, 1999. **117**(6): p. 744-51.
- 373 10. Chauhan, D.S., et al., *Papillofoveal traction in macular hole formation: the*  
374 *role of optical coherence tomography*. Arch Ophthalmol, 2000. **118**(1): p. 32-  
375 8.
- 376 11. Tanner, V., et al., *Optical coherence tomography of the vitreoretinal interface*  
377 *in macular hole formation*. Br J Ophthalmol, 2001. **85**(9): p. 1092-7.
- 378 12. Uemoto, R., et al., *Macular configuration determined by optical coherence*  
379 *tomography after idiopathic macular hole surgery with or without internal*  
380 *limiting membrane peeling*. Br J Ophthalmol, 2002. **86**(11): p. 1240-2.
- 381 13. Gallemore, R.P., et al., *Diagnosis of vitreoretinal adhesions in macular*  
382 *disease with optical coherence tomography*. Retina, 2000. **20**(2): p. 115-20.
- 383 14. Schuman, J.S., et al., *Quantification of nerve fiber layer thickness in normal*  
384 *and glaucomatous eyes using optical coherence tomography*. Arch  
385 Ophthalmol, 1995. **113**(5): p. 586-96.
- 386 15. Fercher, A.F., et al., *Measurement of Intraocular Distances by Backscattering*  
387 *Spectral Interferometry*. Optics Communications, 1995. **117**(1-2): p. 43-48.
- 388 16. Hausler, G. and M.W. Lindner, *"Coherence Radar" and "Spectral Radar"---*  
389 *New Tools for Dermatological Diagnosis*. Journal of Biomedical Optics, 1998.  
390 **3**(1): p. 21-31.
- 391 17. Wojtkowski, M., et al., *In vivo human retinal imaging by Fourier domain*  
392 *optical coherence tomography*. Journal of Biomedical Optics, 2002. **7**(3): p.  
393 457-463.
- 394 18. Leitgeb, R., C. Hitzenberger, and A. Fercher, *Performance of fourier domain*  
395 *vs. time domain optical coherence tomography*. Opt. Express, 2003. **11**(8): p.  
396 889-894.
- 397 19. de Boer, J.F., et al., *Improved signal-to-noise ratio in spectral-domain*  
398 *compared with time-domain optical coherence tomography*. Opt Lett, 2003.  
399 **28**(21): p. 2067-9.

- 400 20. Sander, B., et al., *Enhanced optical coherence tomography imaging by*  
401 *multiple scan averaging*. Br J Ophthalmol, 2005. **89**(2): p. 207-12.
- 402 21. Sakamoto, A., M. Hangai, and N. Yoshimura, *Spectral-domain optical*  
403 *coherence tomography with multiple B-scan averaging for enhanced imaging*  
404 *of retinal diseases*. Ophthalmology, 2008. **115**(6): p. 1071-1078 e7.
- 405 22. Ferguson, R.D., et al., *Tracking optical coherence tomography*. Opt. Lett.,  
406 2004. **29**(18): p. 2139-2141.
- 407 23. Hammer, D.X., et al., *Active retinal tracker for clinical optical coherence*  
408 *tomography systems*. Journal of Biomedical Optics, 2005. **10**(2): p. 024038-  
409 11.
- 410 24. Drexler, W., et al., *In vivo ultrahigh-resolution optical coherence tomography*.  
411 Opt Lett, 1999. **24**(17): p. 1221-3.
- 412 25. Fujimoto, J.G., *Optical coherence tomography for ultrahigh resolution in vivo*  
413 *imaging*. Nat Biotech, 2003. **21**(11): p. 1361-1367.
- 414 26. Ko, T.H., et al., *Comparison of ultrahigh- and standard-resolution optical*  
415 *coherence tomography for imaging macular hole pathology and repair*.  
416 Ophthalmology, 2004. **111**(11): p. 2033-43.
- 417 27. Iwasaki, T., et al., *Three-dimensional optical coherence tomography of*  
418 *proliferative diabetic retinopathy*. Br J Ophthalmol, 2008. **92**(5): p. 713.
- 419 28. Wojtkowski, M., et al., *Three-dimensional retinal imaging with high-speed*  
420 *ultrahigh-resolution optical coherence tomography*. Ophthalmology, 2005.  
421 **112**(10): p. 1734-46.
- 422 29. Schmidt-Erfurth, U., et al., *Three-dimensional ultrahigh-resolution optical*  
423 *coherence tomography of macular diseases*. Invest Ophthalmol Vis Sci, 2005.  
424 **46**(9): p. 3393-402.
- 425 30. Hitzenberger, C., et al., *Three-dimensional imaging of the human retina by*  
426 *high-speed optical coherence tomography*. Opt. Express, 2003. **11**(21): p.  
427 2753-2761.
- 428 31. Götzinger, E., et al., *Retinal pigment epithelium segmentation by polarization*  
429 *sensitive optical coherence tomography*. Opt. Express, 2008. **16**(21): p. 16410-  
430 16422.
- 431 32. Ahlers, C., et al., *Automatic segmentation in three-dimensional analysis of*  
432 *fibrovascular pigment epithelial detachment using high-definition optical*  
433 *coherence tomography*. Br J Ophthalmol, 2008. **92**(2): p. 197-203.
- 434 33. Chan, A., et al., *Quantification of photoreceptor layer thickness in normal*  
435 *eyes using optical coherence tomography*. Retina, 2006. **26**(6): p. 655-60.
- 436 34. Kagemann, L., et al., *Sources of longitudinal variability in optical coherence*  
437 *tomography nerve-fibre layer measurements*. Br J Ophthalmol, 2008. **92**(6): p.  
438 806-9.
- 439 35. Sadda, S.R., et al., *Errors in retinal thickness measurements obtained by*  
440 *optical coherence tomography*. Ophthalmology, 2006. **113**(2): p. 285-93.
- 441 36. Fung, A.E., et al., *An optical coherence tomography-guided, variable dosing*  
442 *regimen with intravitreal ranibizumab (Lucentis) for neovascular age-related*  
443 *macular degeneration*. Am J Ophthalmol, 2007. **143**(4): p. 566-83.
- 444 37. Emerson, G.G., et al., *Optical coherence tomography findings during*  
445 *pegaptanib therapy for neovascular age-related macular degeneration*.  
446 Retina, 2007. **27**(6): p. 724-9.
- 447 38. Ozdemir, H., S.A. Karacorlu, and M. Karacorlu, *Early optical coherence*  
448 *tomography changes after photodynamic therapy in patients with age-related*  
449 *macular degeneration*. Am J Ophthalmol, 2006. **141**(3): p. 574-6.

- 450 39. Coscas, F., et al., *Optical coherence tomography identification of occult*  
451 *choroidal neovascularization in age-related macular degeneration.* Am J  
452 Ophthalmol, 2007. **144**(4): p. 592-9.
- 453 40. Meyer, C.H., et al., *Ranibizumab in Patients with Subfoveal Choroidal*  
454 *Neovascularization Secondary to Age-Related Macular Degeneration. Interim*  
455 *Results from the SUSTAIN trial.* Invest Ophthalmol Vis Sci, 2008. **49**: p. E-  
456 Abstract 273.
- 457 41. Dalton, M. (2008) *Lucentis at one year.* Eyeworld.
- 458 42. Bolz, M. and U. Schmidt-Erfurth, *Ranibizumab EXCITE study: Exploring the*  
459 *Value of Optical Coherence Tomography for the Management of Ranibizumab*  
460 *Therapy in Age-Related Macular Degeneration., in 8th EURETINA Congress.*  
461 2008: Vienna, Austria.
- 462 43. Salinas-Alaman, A., et al., *Using optical coherence tomography to monitor*  
463 *photodynamic therapy in age related macular degeneration.* Am J  
464 Ophthalmol, 2005. **140**(1): p. 23-8.
- 465 44. Krebs, I., et al., *Optical coherence tomography guided retreatment of*  
466 *photodynamic therapy.* Br J Ophthalmol, 2005. **89**(9): p. 1184-7.
- 467 45. Ahlers, C., et al., *Time Course of Morphologic Effects on Different Retinal*  
468 *Compartments after Ranibizumab Therapy in Age-related Macular*  
469 *Degeneration.* Ophthalmology, 2008. **115**(8): p. e39-e46.
- 470 46. Vujosevic, S., et al., *Diabetic macular edema: correlation between*  
471 *microperimetry and optical coherence tomography findings.* Invest  
472 Ophthalmol Vis Sci, 2006. **47**(7): p. 3044-51.
- 473 47. Moutray, T., et al., *Relationships between clinical measures of visual function,*  
474 *fluorescein angiographic and optical coherence tomography features in*  
475 *patients with subfoveal choroidal neovascularisation.* Br J Ophthalmol, 2008.  
476 **92**(3): p. 361-4.
- 477 48. Hangai, M., et al., *Three-dimensional imaging of macular holes with high-*  
478 *speed optical coherence tomography.* Ophthalmology, 2007. **114**(4): p. 763-  
479 73.
- 480 49. Tan, O., et al., *Mapping of macular substructures with optical coherence*  
481 *tomography for glaucoma diagnosis.* Ophthalmology, 2008. **115**(6): p. 949-56.
- 482 50. Drexler, W., et al., *Ultrahigh-resolution ophthalmic optical coherence*  
483 *tomography.* Nature Medicine, 2001. **7**(4): p. 502-507.
- 484 51. Pircher, M., et al., *Retinal cone mosaic imaged with transverse scanning*  
485 *optical coherence tomography.* Optics Letters, 2006. **31**(12): p. 1821-1823.
- 486 52. Miller, D.T., et al. *Coherence gating and adaptive optics in the eye.* in  
487 *Conference on Coherence Domain Optical Methods and Optical Coherence*  
488 *Tomography in Biomedical VII.* 2003. San Jose, Ca.
- 489 53. Hermann, B., et al., *Adaptive-optics ultrahigh-resolution optical coherence*  
490 *tomography.* Optics Letters, 2004. **29**(18): p. 2142-2144.
- 491 54. Zhang, Y., et al., *Adaptive optics parallel spectral domain optical coherence*  
492 *tomography for imaging the living retina.* Optics Express, 2005. **13**(12): p.  
493 4792-4811.
- 494 55. Zawadzki, R.J., et al., *Adaptive-optics optical coherence tomography for high-*  
495 *resolution and high-speed 3D retinal in vivo imaging.* Optics Express, 2005.  
496 **13**(21): p. 8532-8546.
- 497 56. Fernandez, E.J., et al., *Three-dimensional adaptive optics ultrahigh-resolution*  
498 *optical coherence tomography using a liquid crystal spatial light modulator.*  
499 Vision Research, 2005. **45**(28): p. 3432-3444.

- 500 57. Zhang, Y., et al., *High-speed volumetric imaging of cone photoreceptors with*  
501 *adaptive optics spectral-domain optical coherence tomography*. Optics  
502 Express, 2006. **14**(10): p. 4380-4394.
- 503 58. Merino, D., et al., *Adaptive optics enhanced simultaneous en-face optical*  
504 *coherence tomography and scanning laser ophthalmoscopy*. Optics Express,  
505 2006. **14**(8): p. 3345-3353.
- 506 59. Bigelow, C.E., et al., *Compact multimodal adaptive-optics spectral-domain*  
507 *optical coherence tomography instrument for retinal imaging*. Journal of the  
508 Optical Society of America a-Optics Image Science and Vision, 2007. **24**(5):  
509 p. 1327-1336.
- 510 60. Zawadzki, R.J., et al., *Adaptive optics-optical coherence tomography:*  
511 *optimizing visualization of microscopic retinal structures in three dimensions*.  
512 Journal of the Optical Society of America a-Optics Image Science and Vision,  
513 2007. **24**(5): p. 1373-1383.
- 514 61. Pircher, M., et al., *Simultaneous imaging of human cone mosaic with adaptive*  
515 *optics enhanced scanning laser ophthalmoscopy and high-speed transversal*  
516 *scanning optical coherence tomography*. Optics Letters, 2008. **33**(1): p. 22-24.
- 517 62. Hammer, D.X., et al., *Foveal fine structure in retinopathy of prematurity: An*  
518 *adaptive optics Fourier domain optical coherence tomography study*.  
519 Investigative Ophthalmology & Visual Science, 2008. **49**(5): p. 2061-2070.
- 520 63. Choi, S.S., et al., *Changes in cellular structures revealed by ultra-high*  
521 *resolution retinal imaging in optic neuropathies*. Investigative Ophthalmology  
522 & Visual Science, 2008. **49**(5): p. 2103-2119.
- 523 64. Zawadzki, R.J., et al., *Ultrahigh-resolution optical coherence tomography*  
524 *with monochromatic and chromatic aberration correction*. Optics Express,  
525 2008. **16**(11): p. 8126-8143.
- 526 65. Fernandez, E.J., et al., *Ultrahigh resolution optical coherence tomography and*  
527 *pancorrection for cellular imaging of the living human retina*. Optics Express,  
528 2008. **16**(15): p. 11083-11094.
- 529 66. Pircher, M. and R. Zawadzki, *Combining adaptive optics with optical*  
530 *coherence tomography: unveiling the cellular structure of the human retina in*  
531 *vivo*. Expert Rev. Ophthalmol., 2007. **2**(6): p. 1019-1035.
- 532 67. Spaide, R.F., H. Koizumi, and M.C. Pozzoni, *Enhanced depth imaging*  
533 *spectral-domain optical coherence tomography*. Am J Ophthalmol, 2008.  
534 **146**(4): p. 496-500.
- 535 68. Margolis, R. and R.F. Spaide, *A pilot study of enhanced depth imaging optical*  
536 *coherence tomography of the choroid in normal eyes*. Am J Ophthalmol, 2009.  
537 **147**(5): p. 811-5.
- 538 69. Imamura, Y., et al., *Enhanced depth imaging optical coherence tomography of*  
539 *the choroid in central serous chorioretinopathy*. Retina, 2009. **29**(10): p.  
540 1469-73.
- 541 70. Povazay, B., et al., *Enhanced visualization of choroidal vessels using*  
542 *ultrahigh resolution ophthalmic OCT at 1050 nm*. Optics Express, 2003.  
543 **11**(17): p. 1980-1986.
- 544 71. Povazay, B., et al., *Three-dimensional optical coherence tomography at 1050*  
545 *nm versus 800 nm in retinal pathologies: enhanced performance and*  
546 *choroidal penetration in cataract patients*. Journal of Biomedical Optics,  
547 2007. **12**(4): p. 041211.
- 548 72. Lee, E.C., et al., *In vivo optical frequency domain imaging of human retina*  
549 *and choroid*. Opt. Express, 2006. **14**(10): p. 4403-4411.

- 550 73. Yasuno, Y., et al., *In vivo high-contrast imaging of deep posterior eye by 1-um*  
551 *swept source optical coherence tomography and scattering optical coherence*  
552 *angiography*. Opt. Express, 2007. **15**(10): p. 6121-6139.
- 553 74. Srinivasan, V.J., et al., *Ultrahigh-Speed Optical Coherence Tomography for*  
554 *Three-Dimensional and En Face Imaging of the Retina and Optic Nerve Head*.  
555 Investigative Ophthalmology & Visual Science, 2008. **49**(11): p. 5103-5110.
- 556 75. Hee, M.R., et al., *Polarization-sensitive low-coherence reflectometer for*  
557 *birefringence characterization and ranging*. Journal of the Optical Society of  
558 America B-Optical Physics, 1992. **9**(6): p. 903-908.
- 559 76. deBoer, J.F., et al., *Two-dimensional birefringence imaging in biological*  
560 *tissue by polarization-sensitive optical coherence tomography*. Optics Letters,  
561 1997. **22**(12): p. 934-936.
- 562 77. Hitzenberger, C.K., et al., *Measurement and imaging of birefringence and*  
563 *optic axis orientation by phase resolved polarization sensitive optical*  
564 *coherence tomography*. Optics Express, 2001. **9**(13): p. 780-790.
- 565 78. Yasuno, Y., et al., *Birefringence imaging of human skin by polarization-*  
566 *sensitive spectral interferometric optical coherence tomography*. Optics  
567 Letters, 2002. **27**(20): p. 1803-1805.
- 568 79. Götzinger, E., M. Pircher, and C.K. Hitzenberger, *High speed spectral domain*  
569 *polarization sensitive optical coherence tomography of the human retina*.  
570 Optics Express, 2005. **13**(25): p. 10217-10229.
- 571 80. Cense, B., et al., *Polarization-sensitive spectral-domain optical coherence*  
572 *tomography using a single line scan camera*. Optics Express, 2007. **15**(5): p.  
573 2421-2431.
- 574 81. Yamanari, M., et al., *Phase retardation measurement of retinal nerve fiber*  
575 *layer by polarization-sensitive spectral-domain optical coherence tomography*  
576 *and scanning laser polarimetry*. J Biomed Opt, 2008. **13**(1): p. 014013.
- 577 82. Schmitt, J.M. and S.H. Xiang, *Cross-polarized backscatter in optical*  
578 *coherence tomography of biological tissue*. Optics Letters, 1998. **23**(13): p.  
579 1060-1062.
- 580 83. Cense, B., et al., *In vivo depth-resolved birefringence measurements of the*  
581 *human retinal nerve fiber layer by polarization-sensitive optical coherence*  
582 *tomography*. Optics Letters, 2002. **27**(18): p. 1610-1612.
- 583 84. Cense, B., et al., *Thickness and birefringence of healthy retinal nerve fiber*  
584 *layer tissue measured with polarization-sensitive optical coherence*  
585 *tomography*. Investigative Ophthalmology & Visual Science, 2004. **45**(8): p.  
586 2606-2612.
- 587 85. Pircher, M., et al., *Imaging of polarization properties of human retina in vivo*  
588 *with phase resolved transversal PS-OCT*. Optics Express, 2004. **12**(24): p.  
589 5940-5951.
- 590 86. Pircher, M., et al., *Human macula investigated in vivo with polarization-*  
591 *sensitive optical coherence tomography*. Investigative Ophthalmology &  
592 Visual Science, 2006. **47**(12): p. 5487-5494.
- 593 87. Michels, S., et al., *Value of polarisation-sensitive optical coherence*  
594 *tomography in diseases affecting the retinal pigment epithelium*. British  
595 Journal of Ophthalmology, 2008. **92**(2): p. 204-209.
- 596 88. Gotzinger, E., et al., *Three-dimensional polarization sensitive OCT imaging*  
597 *and interactive display of the human retina*. Opt Express, 2009. **17**(5): p.  
598 4151-65.

- 599 89. Fortune, B., G.A. Cull, and C.F. Burgoyne, *Relative Course of Retinal Nerve*  
600 *Fiber Layer Birefringence and Thickness and Retinal Function Changes after*  
601 *Optic Nerve Transection*. Investigative Ophthalmology & Visual Science,  
602 2008. **49**(10): p. 4444-4452.
- 603 90. Götzinger, E., et al., *Retinal nerve fiber layer birefringence evaluated with*  
604 *polarization sensitive spectral domain OCT and scanning laser polarimetry: A*  
605 *comparison*. Journal of Biophotonics, 2008. **1**(2): p. 129-139.
- 606 91. Mujat, M., et al., *Autocalibration of spectral-domain optical coherence*  
607 *tomography spectrometers for in vivo quantitative retinal nerve fiber layer*  
608 *birefringence determination*. J Biomed Opt, 2007. **12**(4): p. 041205.
- 609 92. Miura, M., et al., *Imaging polarimetry in age-related macular degeneration*.  
610 Investigative Ophthalmology & Visual Science, 2008. **49**(6): p. 2661-2667.
- 611 93. Wang, X.J., T.E. Milner, and J.S. Nelson, *Characterization of fluid-flow*  
612 *velocity by optical Doppler tomography*. Optics Letters, 1995. **20**(11): p.  
613 1337-1339.
- 614 94. Yazdanfar, S., A.M. Rollins, and J.A. Izatt, *Imaging and velocimetry of the*  
615 *human retinal circulation with color Doppler optical coherence tomography*.  
616 Opt. Lett., 2000. **25**(19): p. 1448-1450.
- 617 95. Chen, Z., et al., *Noninvasive imaging of in vivo blood flow velocity using*  
618 *optical Doppler tomography*. Opt. Lett., 1997. **22**(14): p. 1119-1121.
- 619 96. Leitgeb, R.A., et al., *Real-time assessment of retinal blood flow with ultrafast*  
620 *acquisition by color Doppler Fourier domain optical coherence tomography*.  
621 Optics Express, 2003. **11**(23): p. 3116-3121.
- 622 97. White, B.R., et al., *In vivo dynamic human retinal blood flow imaging using*  
623 *ultra-high-speed spectral domain optical Doppler tomography*. Optics  
624 Express, 2003. **11**(25): p. 3490-3497.
- 625 98. Makita, S., et al., *Optical coherence angiography*. Optics Express, 2006.  
626 **14**(17): p. 7821-7840.
- 627 99. Hong, Y., et al., *Three-dimensional visualization of choroidal vessels by using*  
628 *standard and ultra-high resolution scattering optical coherence angiography*.  
629 Optics Express, 2007. **15**(12): p. 7538-7550.
- 630 100. Wang, Y.M., et al., *In vivo total retinal blood flow measurement by Fourier*  
631 *domain Doppler optical coherence tomography*. Journal of Biomedical Optics,  
632 2007. **12**(4): p. 041215.
- 633 101. Wehbe, H., et al., *Automatic retinal blood flow calculation using spectral*  
634 *domain optical coherence tomography*. Optics Express, 2007. **15**(23): p.  
635 15193-15206.
- 636 102. Werkmeister, R.M., et al., *Bidirectional Doppler Fourier-domain optical*  
637 *coherence tomography for measurement of absolute flow velocities in human*  
638 *retinal vessels*. Optics Letters, 2008. **33**(24): p. 2967-2969.
- 639 103. Wang, Y., et al., *Measurement of total blood flow in the normal human retina*  
640 *using Doppler Fourier-domain optical coherence tomography*. Br J  
641 Ophthalmol, 2009. **93**(5): p. 634-7.
- 642 104. Bachmann, A.H., et al., *Resonant Doppler flow imaging and optical*  
643 *vivisection of retinal blood vessels*. Optics Express, 2007. **15**(2): p. 408-422.
- 644 105. Wang, R.K., et al., *Three dimensional optical angiography*. Optics Express,  
645 2007. **15**(7): p. 4083-4097.
- 646 106. Michaely, R., et al., *Vectorial reconstruction of retinal blood flow in three*  
647 *dimensions measured with high resolution resonant Doppler Fourier domain*

648 *optical coherence tomography*. Journal of Biomedical Optics, 2007. **12**(4): p.  
649 041213.  
650  
651  
652  
653

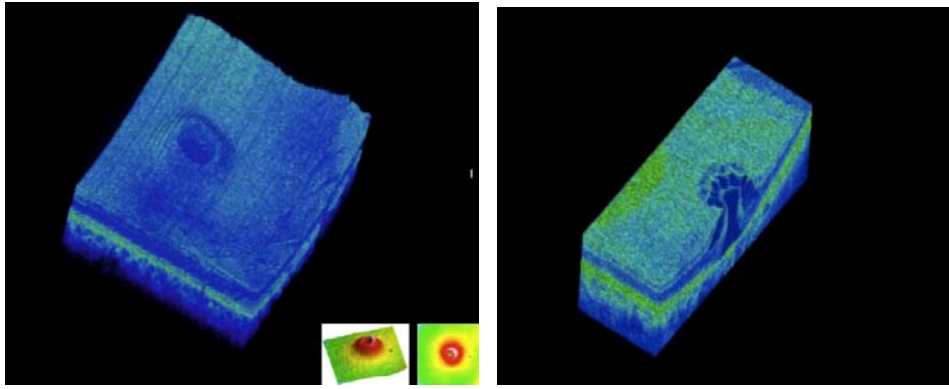


**Figure 1.**

Three-dimensional rendering of a full-thickness macular hole. Images gratefully provided by Christian Ahlers, MD.

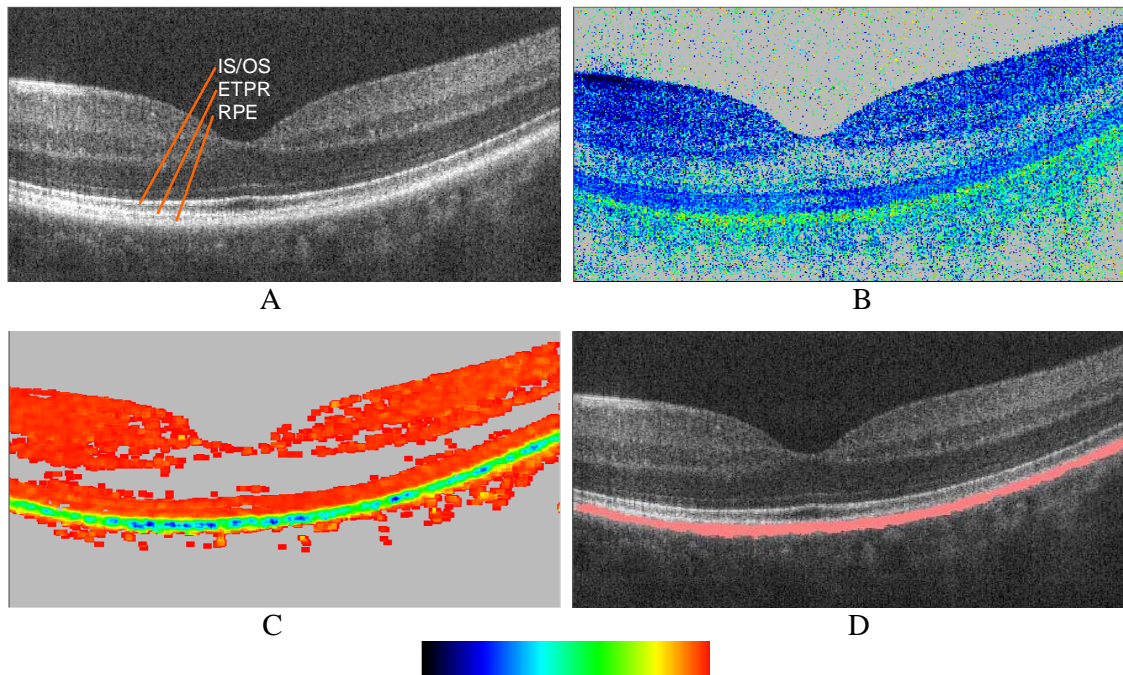


**Figure 2.**

PS-OCT B-scan images of healthy human fovea in vivo. (A) Intensity (log scale); (B) retardation (color bar:  $0^\circ$  -  $90^\circ$ ); (C) degree of polarization uniformity DOPU (color bar: 0 – 1). (D) overlay of intensity image with RPE segmented by DOPU data (red). Image size:  $15^\circ$  (horizontal)  $\times$  0.75 mm (vertical, optical distance). (From E. Götzinger et al.<sup>31</sup> by permission of the Optical Society of America).

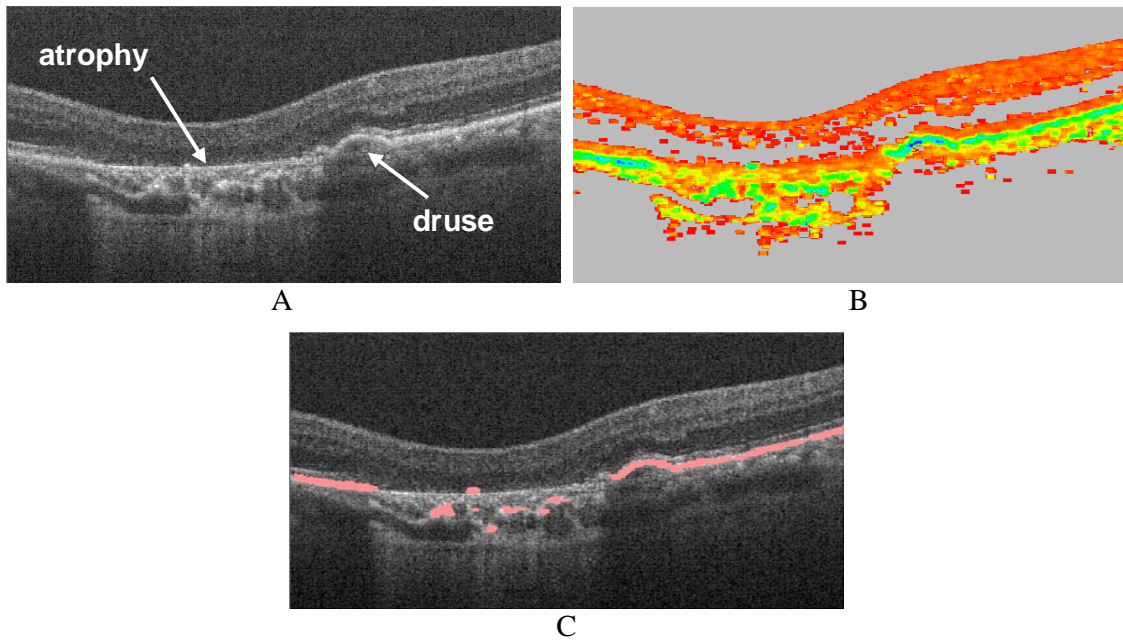


**Figure 3.**

PS-OCT images of retina with AMD. (A) Intensity; (B) DOPU (color bar: see fig 1C); (C) intensity overlaid with segmented RPE. Image size:  $15^\circ$  (horizontal) x 1 mm (vertical). (From E. Göttinger et al.<sup>31</sup> by permission of the Optical Society of America).